Fragment Complementation Studies of Protein Stabilization by Hydrophobic Core Residues†

Tord Berggård,‡,§ Karin Julenius,‡,∥ Andrea Ogard,⊥ Torbjörn Drakenberg, and Sara Linse*

Physical Chemistry 2, Chemical Centre, University of Lund, S-221 00 Lund, Sweden

Received June 28, 2000; Revised Manuscript Received October 11, 2000

ABSTRACT: Interactions that stabilize the native state of a protein have been studied by measuring the affinity between subdomain fragments with and without site-specific residue substitutions. A calbindin D_{9k} variant with a single CNBr cleavage site at position 43 between its two EF-hand subdomains was used as a starting point for the study. Into this variant were introduced 11 site-specific substitutions involving hydrophobic core residues at the interface between the two EF-hands. The mutants were cleaved with CNBr to produce wild-type and mutated single-EF-hand fragments: EF1 (residues 1−43) and EF2 (residues 44−75). The interaction between the two EF-hands was studied using surface plasmon resonance (SPR) technology, which follows the rates of association and dissociation of the complex. Wild-type EF1 was immobilized on a dextran matrix, and the wild-type and mutated versions of EF2 were injected at several different concentrations. In another set of experiments, wild-type EF2 was immobilized and wild-type or mutant EF1 was injected. Dissociation rate constants ranged between 1.1×10^{-5} and 1.0×10^{-2} s^{-1} and the association rate constants between 2×10^5 and 4.0×10^6 M^{-1} s^{-1}. The affinity between EF1 and EF2 was as high as 3.6×10^{11} M^{-1} when none of them was mutated. For the 11 hydrophobic core mutants, a strong correlation ($r = 0.999$) was found between the affinity of EF1 for EF2 and the stability toward denaturation of the corresponding intact protein. The observed correlation implies that the factors governing the stability of the intact protein also contribute to the affinity of the bimolecular EF1−EF2 complex. In addition, the data presented here show that interactions among hydrophobic core residues are major contributors both to the affinity between the two EF-hand subdomains and to the stability of the intact domain.

The native structures of proteins are governed by their amino acid sequences, yet dependent on multiple, noncovalent interactions. These include hydrogen bonds, electrostatic interactions, van der Vaals forces, and the hydrophobic effect. The relative importance of different nonbonded interactions for the stability of a protein is hard to assess since the forces in the native state must be compared to the forces in the unfolded form, and also interactions with the solvent in the two states need to be considered. The development of reliable prediction methods for protein structure and stability is dependent on the availability of accurate experimental data on the contributions of different types of interactions, for example, those involving the large hydrophobic groups in protein cores.

Hydrophobic cores of proteins have been discussed as everything from solid-like rigid structures to fluid-like oily compartments. A recent survey of 100 well-resolved crystal structures shows an impressively well-fitted packing in protein interiors with the side chains neatly interlocked (*1*). This is in apparent conflict with a molecular dynamics (MD) simulation suggesting that the side chains in the interior are packed more like nuts and bolts in a jar than jigsaw puzzle pieces (*2*). MD simulations point to a high frequency of ring flips and hopping of leucine side chains, suggesting a fluid-like interior with low energy barriers to such motions (*3*). Spectroscopic studies show restricted motion for some aromatics and free rotation for others, suggesting that the flexibility of the packing may vary from protein to protein and also between different regions of the same protein (*4*). A recent phage display study points to a highly specific packing of neatly interlocked hydrophobic side chains in calmodulin (*5*).

On the basis of studies of barnase, it has been argued that every CH_2 group in the hydrophobic core contributes equally (4.5 kJ mol^{-1}) to the net stability of a protein (*6*), which would imply that the core is plastic and adjustable. An overview of a large number of mutants from several proteins implied that the hydrophobic core in general is fairly rigid, since both the increase and decrease of hydrophobic side chain volume on average lead to destabilization (*7*). Reconstitution studies have greatly enhanced our understanding of

† This work was supported by grants from the Swedish Natural Science Research Council (NFR, to S.L.), the Swedish National Council for Medical Research (MFR, to S.L. and T.D.), and a postdoctoral stipend from Salubrin/Druvan AB (T.B.).

* To whom correspondence should be addressed: Physical Chemistry 2, Chemical Centre, University of Lund, S-221 00 Lund, Sweden. Telephone: +46-46-2228246. Fax: +46-46-2224543. E-mail: Sara.Linse@fkem2.lth.se.

‡ These authors contributed equally.

§ Current address: Department of Physiology and Biophysics, VTMB, 301 University Blvd., Galveston, TX 77555.

∥ Current address: Bioinvent AB, S-221 00 Lund, Sweden.

⊥ Current address: Bioglan AB, Box 50310, S-202 13 Malmö, Sweden.

10.1021/bi0014812 CCC: $20.00
Published on Web 01/10/2001

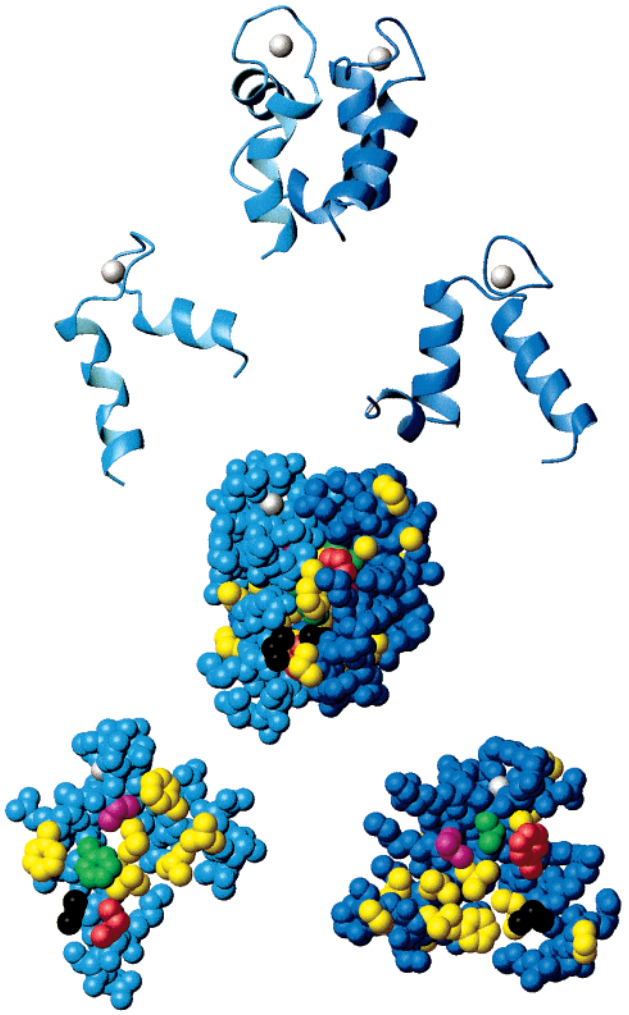

FIGURE 1: Three-dimensional structure of Ca^{2+}-saturated calbindin D_{9k} based on the X-ray structure coordinates (*21*) (PDB entry 4icb). EF1 and EF2 are shown in dark and light blue, respectively. The first and third row from the top show the intact protein, while the second and fourth rows show fragments EF1 (right) and EF2 (left) rotated 90° to the right and left, respectively, to show the inter-EF-hand surfaces. The ribbon structures in rows 1 and 2 are shown in the same orientations as the space filling models in rows 3 and 4, respectively. Leu28 and Val61 are shown in magenta, Leu23 and Phe66 in green, Leu6 and Val70 in black, and Phe10 and Ile73 in red. Other hydrophobic side chains are shown in yellow and Ca^{2+} ions in silver. The picture was generated using MolMol (*22*).

intraprotein interactions and have shown that the cores of many proteins are specifically packed, allowing for fragment complexes to reproduce the native three-dimensional structures and functions (*23*, *24*).

The relative importance of different nonbonded interactions for the stability of a protein is difficult to assess in aqueous solutions, because a very small fraction of the protein is present in the unfolded state. Much of our knowledge about factors governing protein stability is, hence, based on extrapolations from conditions under which both the native and unfolded state are significantly populated, for example, at very high concentration of denaturants. This study is an attempt to overcome this obstacle by studying the role of hydrophobic core substitutions on the reconstitution of a protein from subdomain fragments. For this purpose, we have chosen a small ($M_r \approx 8500$) Ca^{2+}-binding protein of the EF-hand family (*8*), calbindin D_{9k} (Figure 1). The protein has no disulfide bonds and contains two EF-hand helix−loop−helix subdomains. The effect of mutations of hydrophobic core amino acids on the affinity between the two EF-hands in calbindin D_{9k} is measured using surface plasmon resonance (SPR)[1] technology, and compared to the earlier reported effects on the stability of the intact protein (*7*, *9*). A strong correlation is found between the affinity and stability, implying that fragment complementation studies may be valuable in assessing the relative importance of different interactions that stabilize the native states of proteins.

EXPERIMENTAL PROCEDURES

Protein Mutagenesis and Purification. The mutant proteins derived from bovine calbindin D_{9k} were expressed in *Escherichia coli* from synthetic genes, produced by cassette mutagenesis, and purified as described previously (*10*, *11*). Agarose gel electrophoresis, SDS−polyacrylamide gel electrophoresis, isoelectric focusing, and ^{1}H NMR spectroscopy confirmed the purity.

CNBr Cleavage and Fragment Purification. Cleavage at the methionine residues at positions 0 and 43 with CNBr and purification of the resulting fragments with ion exchange chromatography were performed as follows. Fifty milligrams of calbindin D_{9k} (with Pro43 → Met or hydrophobic + Pro43 → Met substitution) was dissolved in 1.2 mL of doubly distilled H_2O and put on ice. TFA (4.8 mL) was added gradually on ice with gentle shaking. The protein/TFA solution was added to 0.6 g of CNBr on ice, and N_2 gas was bubbled through for 5 min. The sample was sealed and left at room temperature overnight, followed by evaporation using a Buchi rotavapor. The sample was redissolved in 30 mL of 5 mM EDTA, and the pH was adjusted to 7.5 using 1 M Tris base (final Tris concentration of ∼24 mM). The sample was pumped onto a 1.5 cm × 12 cm DEAE-Sephacel column pre-equilibrated in 10 mM Tris/HCl and 1 mM EDTA (pH 7.5). The sample was eluted with a linear NaCl gradient from 0.05 to 0.40 M. The identity and purity of the fragments was readily confirmed by agarose gel electrophoresis, because EF1 has a very low mobility and EF2 has a higher mobility than residual intact protein (*15*). EF1 (residues 1−43) eluted in the loading wash, while EF2 (residues 44−75) eluted late in the gradient, in two pools corresponding to monomeric and dimeric material, respectively. Remaining uncleaved protein eluted before EF2.

Agarose Gel Electrophoresis. Agarose gel electrophoresis was carried out in sodium barbitone buffer (pH 8.6) using a 1% agarose gel. Either 2 mM EDTA or 2 mM $CaCl_2$ was included in the buffer. The protein was visualized by staining with Coomassie blue.

Materials. All chemicals were of the highest grade commercially available. The CM5 sensor chips and amine coupling kit containing *N*-hydroxysuccinimide (NHS), *N*-ethyl-*N*′-(dimethylaminopropyl)carbodiimide (EDC), and ethanolamine hydrocloride were from Pharmacia Biosensor AB (Uppsala, Sweden). The surfactant Tween 20 was from

[1] Abbreviations: SPR, surface plasmon resonance; EF1, fragment with residues 1−43 of calbindin D_{9k}; EF2, fragment with residues 44−75 of calbindin D_{9k}; EDTA, ethylenedinitrilotetraacetic acid disodium salt dihydrate; SDS, sodium dodecyl sulfate; PAGE, polyacrylamide gel electrophoresis; Tris, tris(hydroxymethyl)aminomethane.

Riedel de Haen (Seelze, Holland). The EDTA solution was made from Titriplex III from Merck (Darmstadt, Germany), and the pH was adjusted using KOH.

Surface Plasmon Resonance Studies. The interaction between EF1 and EF2 (without or with mutation in one of them) was studied by surface plasmon resonance technology, using a BIAcore biosensor system (Pharmacia Biosensor AB). As a flow buffer, 10 mM HEPES/KOH (pH 7.4) with 0.15 M NaCl, 0.005% Tween 20, 0.02% NaN_3, and either 2 mM $CaCl_2$ or 3.4 mM EDTA was used. The small amount of Tween 20 in the buffers was used to prevent clogging of the tubes in the BIAcore apparatus. All buffers were filtered through sterile 0.22 μm filters before use. The built-in thermostat kept the temperature at 25.0 °C during all experiments.

Immobilization of EF1 or EF2 to the sensor chip was performed at a constant flow rate of 5 μL/min, using the EDTA-containing flow buffer. Equal volumes of 0.1 M NHS and 0.4 M EDC were first mixed, and 40 μL of the mixture was allowed to flow over the sensor chip surface to activate the carboxymethylated dextran (8 min). Forty-five microliters of 1 mg/mL EF1 or EF2 in 10 mM NaAc at pH 4.5 (EF1) or pH 3.5 (EF2) was then injected over the sensor chip (9 min), after which unreacted NHS ester groups were deactivated by 20 μL of 1.0 M ethanolamine hydrochloride (pH 8.5, 4 min). The system was regenerated by 10 μL of 10 mM EDTA (pH 8, 2 min), to remove all noncovalently bound molecules. No immobilization was used for more than 2 weeks.

EF1 association to and dissociation from the immobilized EF2 were studied at several different EF1 concentrations ranging from 0.31 nM to 10 μM. EF2 association to and dissociation from the immobilized EF1 were studied at several different EF2 concentrations ranging from 0.5 to 20 μM. The Ca^{2+}-containing flow buffer was used for both association and dissociation kinetics, except for one set of experiments where the EDTA-containing flow buffer was used to check for non-Ca^{2+}-dependent binding. Protein stock solutions were diluted to different concentrations using the flow buffer, and 45 μL was injected during the association phase at a constant flow rate of 3 μL/min. The association phase was followed for 15 min and the dissociation phase for various lengths of time, from 30 min to 27 h. The dissociation phase was studied at a constant flow rate of 3 or 15 μL/min. The higher flow rate reduced the signal-to-noise ratio, but the observed dissociation rate constants were not affected. After each experiment cycle, 10 mM EDTA (pH 8) was injected for 2 min to remove residual associated fragments. For the wild type, L6V, F66W, V70L, and I73V, 27 h was not enough to study the complete dissociation, but instabilities in the instrumentation and limitations to the available instrument time made it difficult to study the dissociation for more than 27 h.

Control experiments were performed to confirm that the binding was specific. Intact calbindin D_{9k} was immobilized to the dextran matrix of a flow cell using the same immobilization procedure as described above, and another flow cell was prepared for a blank control by the same treatment, but using NaAc buffer containing no protein in the coupling step. Experiments for binding of EF1 or EF2 to the blank cell and to the intact protein cell were performed in the same way as those for the surface immobilized with EF1 or EF2, but no binding was detected.

Data Analysis. The data were evaluated using a nonlinear least-squares analysis method, as suggested by O'Shannessy (*12*, *13*). The data analysis was carried out using the software MATLAB (The Math Works, Inc.). A MATLAB program was written using the Levenberg−Marquardt algorithm for least-squares fits (*14*). The program, called LMFIT, allows simultaneous fitting of an unlimited number of functions and data sets so that one or more common constants may be determined with higher precision.

The association reaction studied by using SPR occurs between component B (here EF1 or EF2) immobilized to the gold dextran-coated sensor chip surface and component A in solution (here the different EF1 and EF2 fragments). Component A is in constant flow (constant concentration and constant flow rate) during the association phase, and A−B complex formation leads to a change in the refractive index of the sensor chip surface, which is reported continuously in terms of response units (RU). The response is proportional to the total mass of the molecules bound at the surface. The dissociation process is initiated by change to a constant flow of protein-free buffer, and a decrease in the response corresponds to component A dissociating from the immobilized component B into the mobile phase. In addition to the response changes due to association and dissociation of component A, the signal changes abruptly when protein injection starts or ends, due to changes in refractive index, so the first and the last few points of each phase are omitted in the fitting procedure.

Dissociation Kinetics. The dissociation phase was analyzed using first-order kinetics, in which the SPR response $R(t)$ is given by the following equation

$$R(t) = C \exp(-k_{off}t) + R_0 \quad (1)$$

where k_{off} is the dissociation rate constant, C is $R(t=0) - R_0$, and R_0 is the baseline value. The SPR response approaches R_0 when t approaches infinity. Several data sets were used simultaneously to obtain better precision in the dissociation rate constants using the multiple-function option in LMFIT. For each mutant, R_0 and C were allowed to be curve-specific.

Association Kinetics. Since the flow of the mobile phase is fast compared to the association and dissociation reactions, it is assumed that the concentration of A is held constant in the flow cell during the entire association phase. The SPR signal during the association phase can then be described by the equation

$$R(t) = R_0 + R_{eq}\{1 - \exp[-([A]k_{on} + k_{off})t]\} \quad (2)$$

in which k_{on} is the association rate constant and R_0 is the SPR value at time 0. R_0 is generally not the same as the baseline value, due to the sensitivity of the SPR to changes in solvent composition. The values of the dissociation rate constants obtained from the analysis of the dissociation phase were used as k_{off}. The SPR value approaches $R_0 + R_{eq}$ when t approaches infinity. R_{eq} is equal to

$$R_{eq} = \frac{R_{max}[A]k_{on}}{[A]k_{on} + k_{off}} \quad (3)$$

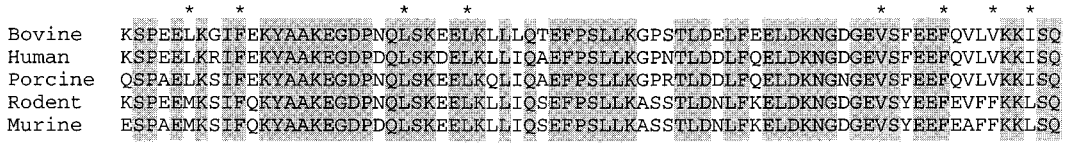

FIGURE 2: Sequence alignment of human, bovine, porcine, rodent, and murine calbindin D_{9k}. Amino acid residues that are conserved in all species are shaded. Mutated residues are indicated with an asterisk.

where R_{max} is the maximum SPR response, which would be observed if EF1 or EF2 were bound to all the available molecules on the surface (some of the immobilized fragment may not be available for binding due to the unsuitable geometry of the immobilization). R_{max} would in principle be constant for all association experiments run on one particular surface of immobilized EF1 or EF2. Alas, instabilities in the instrument and the deterioration of the immobilized protein with time and number of experiments may cause variations in R_{max}.

For EF2 binding to immobilized EF1, no acceptable fits could be obtained using eq 2. An attempt was therefore made to take into account the possibility that the injected EF2 is partly dimerized, while only monomeric EF2 would bind to EF1. The concentration of free EF2 monomer ([A]) is given by

$$K_{A_2} = \frac{[A_2]}{[A]^2} \quad (4)$$

where K_{A_2} is the dimerization constant of the EF2 homodimer. The total amount of EF2, A_{tot}, in the mobile phase is known:

$$A_{tot} = [A] + 2[A_2] \quad (5)$$

Equations 4 and 5 can be combined to yield the following quadratic equation with [A] as the only unknown:

$$2K_{A_2}[A]^2 + [A] - A_{tot} = 0 \quad (6)$$

Equation 6 is easily solved using the standard solution for quadratic equations:

$$[A] = -\frac{1}{4K_{A_2}} + \sqrt{\frac{1}{16K_{A_2}^2} + \frac{A_{tot}}{2K_{A_2}}} \quad (7)$$

For a certain EF2 fragment, association curves measured at 10 or 11 different total concentrations were fitted simultaneously to eq 2 with the expression in eq 7 used for [A] and the expression in eq 3 used for R_{eq}. The values of the dissociation rate constants obtained from the analysis of the dissociation phase were used as k_{off}. R_0 and R_{eq} were allowed to be curve-specific, and K_d and k_{on} were the same for all curves.

We also tried fitting the association curves of each EF2 fragment to a simple, non-concentration-dependent exponential:

$$R(t) = R_0 + R_{eq}[1 - \exp(-k_{app}t)] \quad (8)$$

$R(t)$ approaches the equilibrium value $R_0 + R_{eq}$ when t approaches infinity. R_0 and R_{eq} were allowed to be curve-specific, and k_{app} was the same for all curves.

Fluorescence Spectroscopy. Fluorescence spectra were recorded in quartz cuvettes between 310 and 450 nm using a Perkin-Elmer LS-50B spectrofluorometer. The association of EF2 and EF1 was studied using either the Tyr in EF1 (excitation at 280 nm) or the Trp in F66W-EF2 (excitation at 295) as a reporter of complex formation. In the first case, a solution of 0.1 μM wt-EF1 in 20 mM Tris/HCl, 150 mM KCl, and 1 mM $CaCl_2$ (pH 7.5) was titrated with wt-EF2 from a concentrated stock solution and the Tyr fluorescence recorded. In the second case, a solution of 0.1 μM F66W-EF2 in 20 mM Tris/HCl, 150 mM KCl, and 1 mM $CaCl_2$ (pH 7.5) was titrated with wt-EF1 from a concentrated stock solution and the Trp fluorescence recorded. The ability of different EF2 mutants to compete with F66W-EF2 for binding to wt-EF1 was studied using a mixture of 1 μM F66W-EF2 and 1 μM wt-EF1 and increasing concentrations of the competing EF2 variant, using Trp fluorescence as a reporter of the amount of heterodimer complex containing F66W-EF2.

RESULTS

Mutagenesis and Nomenclature. Eleven site-specific substitutions involving eight hydrophobic core residues at the interface between the two EF-hands of calbindin D_{9k} were introduced to produce 11 mutants. Five of the substitutions were made in the N-terminal EF-hand and six in the C-terminal EF-hand at the positions highlighted in Figures 1 and 2. The substitutions were introduced into a mutated version of the minor A form of bovine calbindin D_{9k} in which Met43 is substituted for Pro43 in the loop between the two EF-hands. The mutants are named after their hydrophobic substitutions using one-letter amino acid codes. Hence, in addition to the substitution Pro43 → Met, L6V contains the substitution Leu6 → Val, F10A Phe10 → Ala, L23A Leu23 → Ala, L23G Leu23 → Gly, L28A Leu28 → Ala, V61A Val61 → Ala, V61G Val61 → Gly, F66A Phe66 → Ala, F66W Phe66 → Trp, V70L Val70 → Leu, and I73V Ile73 → Val.

CNBr Cleavage and Isolation of Fragments. Each hydrophobic core mutant was cleaved by CNBr to produce single-EF-hand fragments EF1 (residues 1−43) and EF2 (residues 44−75). The two fragments have different net charges (−1 for EF1 and −6 for EF2) and can be separated from each other using ion exchange chromatography in the presence of EDTA (*15*, *16*). In the calcium-bound state, the two EF-hands interact so tightly that they resist separation by this method (*15*, *26*). From each mutant protein were derived either wild-type EF1 and mutant EF2 or mutant EF1 and wild-type EF2. Typical yields of pure fragment were 16−19 mg of EF1 and 8−12 mg of EF2 when 50 mg of intact protein was cleaved.

Surface Plasmon Resonance Studies. The wild-type and mutated EF-hand fragments were used in surface plasmon resonance (SPR) studies of the association and dissociation

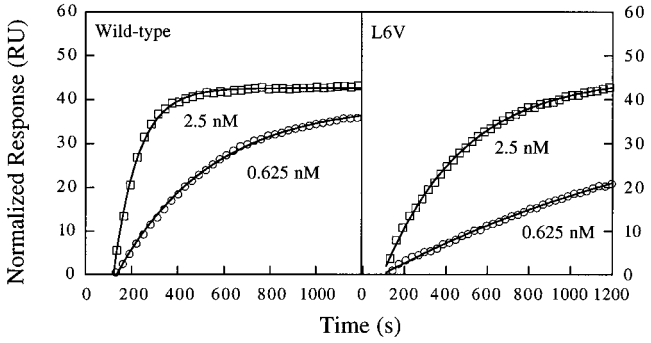

FIGURE 3: Surface plasmon resonance studies of the association between EF1 and immobilized EF2. The sensorgrams show the interaction of wild-type or L6V EF1 with immobilized EF2. Computer fits to sensorgram data are shown as solid lines. The concentrations of the analyte in flow phase during the association phase are indicated next to each curve.

processes between the two EF-hands. Wild-type EF1 and wild-type EF2 were immobilized to separate activated dextran matrixes on BIAcore sensor chip gold surfaces using amine coupling. The amount of immobilized fragment was usually around 1 ng/mm^2 (1000 RU) for EF1 and 0.3 ng/mm^2 for EF2. The wild-type or mutated versions of the complementary EF-hand were injected at different concentrations ranging from 0.3 nM to 25 μM. Association to the immobilized component was assessed for 15 min, and the dissociation into flow buffer was followed for 2−27 h depending on the off rate.

EF1 Binding to Immobilized EF2. The interaction between immobilized EF2 and wild-type or mutated EF1 was studied at 11 different EF1 concentrations ranging from 0.31 nM to 10 μM. Examples of association phase SPR response are shown in Figure 3, and the dissociation curves for all EF1-fragments are shown in Figure 4A. The low signal at saturation (~50 RU) suggests that a large fraction of the immobilized EF2 is incapable of binding EF1. The mutants can be grouped into three categories according to their dissociation response: L23G and F10A are almost completely dissociated from the immobilized EF2 within a few minutes, L28A and L23A display a comparatively slower dissociation process with a half-life of ~10 min, while the wild-type and L6V dissociate much slower with a half-life of ~1 day. For each EF1 mutant, eq 1 was fitted to the different dissociation curves (Table 1). In all cases, the dissociation rate constants were found not to be concentration-dependent, except for those of L23G and F10A at concentrations of <200 nM where the signal was so low that instrumental drift perturbed the curves.

The association curves of wild-type EF1, L6V, F10A, L23A, and L28A are concentration-dependent, and in all cases, the k_{on} values obtained by computer fitting eq 2 to the data are very similar for concentrations in the range of 0.6−20 nM (Figure 3). At higher concentrations of EF1, the on rate (k_{on}[A]) becomes too high for accurate determination of the association rate constant (k_{on}). On the basis of the values of k_{on} and k_{off}, the equilibrium association constant K_A for the wild type is 3.5×10^{11} M^{-1}. The affinity is reduced by a factor of 9 for L6V and by a factor of 700−20000 for the other mutants (Table 1).

EF2 Binding to Immobilized EF1. The interaction between immobilized EF1 and wild-type or mutated EF2 was studied

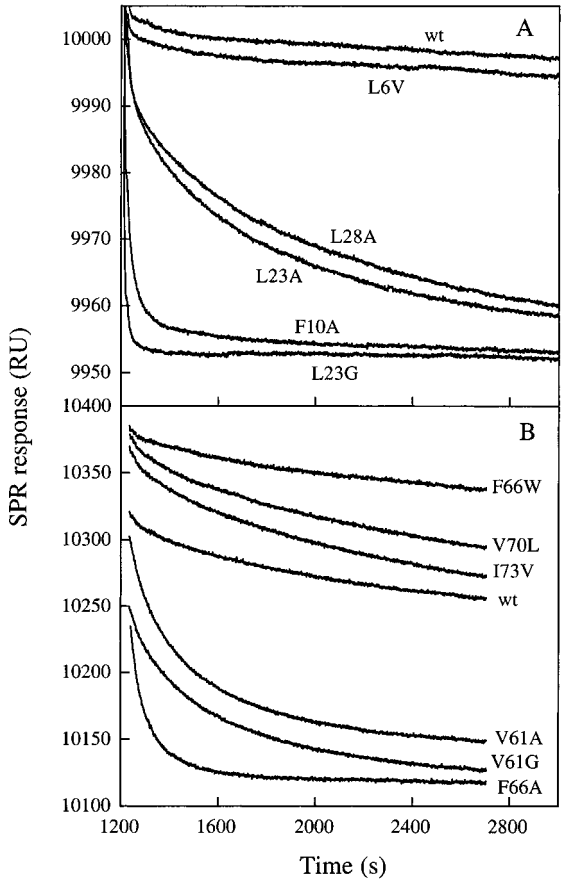

FIGURE 4: Dissociation phase as monitored by surface plasmon resonance (SPR) for EF2 or EF1 fragments with different amino acid substitutions. EF1 or EF2 is immobilized on a dextran matrix. The sensorgrams show the dissociation phase of (A) EF2 and EF2 mutants with immobilized EF1 and (B) EF1 and EF1 mutants with immobilized EF2, injected at a concentration of 0.5 μM.

Table 1: Dissociation and Association Rates for EF1 Interacting with Immobilized EF2[a]

	k_{off} (s^{-1})[b]	k_{on} (M^{-1} s^{-1})[c]	K_A (M^{-1})[d]
wild type	1.1×10^{-5}	4.0×10^{6}	3.6×10^{11}
L6V	2.2×10^{-5}	9.4×10^{5}	4.3×10^{10}
F10A	3.1×10^{-3}	2×10^{5}	6×10^{7}
L23A	1.6×10^{-3}	8×10^{5}	5×10^{8}
L23G	1.0×10^{-2}	$<2 \times 10^{5}$	$<2 \times 10^{7}$
L28A	1.1×10^{-3}	8×10^{5}	7×10^{8}

[a] Obtained by fitting to SPR data as described in Data Analysis. Errors estimated as one standard deviation are generally less than 4%; otherwise, only one significant digit is given. [b] From eq 1. [c] From eq 2. [d] Calculated as $K_A = k_{on}/k_{off}$.

at 11 different EF2 concentrations ranging from 0.5 to 20 μM. Examples of association phase SPR responses are shown in Figure 5, and the dissociation curves for all EF2 fragments are shown in Figure 4B. The low signal at saturation (~150 RU) suggests that a large fraction of the immobilized EF1 is incapable of binding EF2. It is clear from the raw data that the dissociation rate varies substantially between the different mutants. F66A, V61G, and V61A are almost completely dissociated from the immobilized EF1 after 30 min, while the dissociation of the wild type, F66W, V70L, and I73V has only just begun. The dissociation rate constants were found not to be concentration-dependent. For each EF2 mutant, eq 1 was fitted simultaneously to the different dissociation curves. The resulting dissociation rate constants

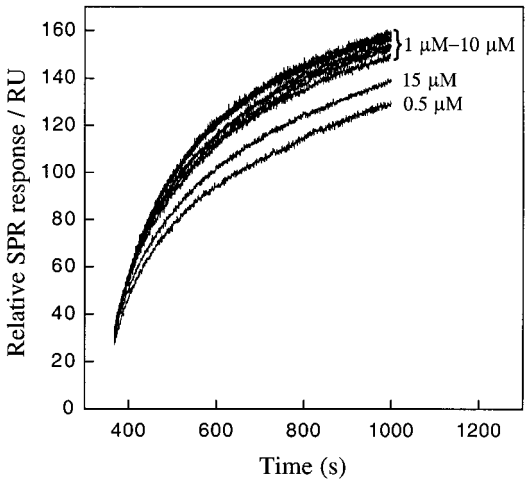

FIGURE 5: EF1−EF2 association phase of wild-type EF2 as monitored by surface plasmon resonance (SPR). EF1 is immobilized on a dextran matrix. EF2 is dissolved in the flow buffer at concentrations ranging from 0.5 to 15 μM.

Table 2: Dissociation Rates and Apparent Association Rates for EF2 Interacting with Immobilized EF1[a]

	k_{off} (s^{-1})[b]	k_{app} (s^{-1})[c]		k_{off} (s^{-1})[b]	k_{app} (s^{-1})[c]
wild type	4.0×10^{-5}	4.5×10^{-3}	F66W	2.3×10^{-5}	4.6×10^{-3}
V61G	1.5×10^{-3}	4.2×10^{-3}	V70L	3.7×10^{-5}	4.6×10^{-3}
V61A	3.2×10^{-3}	4.2×10^{-3}	I73V	5.8×10^{-5}	4.7×10^{-3}
F66A	8.8×10^{-3}	6.0×10^{-3}			

[a] Fitted according to methods described in Data Analysis. Errors estimated as one standard deviation are generally less than 2%. [b] From eq 1. [c] From eq 8.

are shown in Table 2.

The relative SPR response during the association phase of wild-type EF2, as shown in Figure 5, clearly does not show the expected concentration dependence. Attempts were made to fit eq 2, or eq 2 combined with eq 7, to the association data of the different mutant EF2 fragments as described in Data Analysis, but no minima were found. The association phase seemed to be independent of concentration and, hence, governed by a rate-limiting step, which is not the association process itself. We therefore tried fitting eq 8 to the data. This was successful, yielding fits with very low final values of χ^2. The resulting apparent association rate constants, k_{app}, are shown in Table 2 and are $\sim 4.5 \times 10^{-3}$ s^{-1} for the wild type and all mutants. For the wild type, this is much lower than the product [EF2]k_{on}, which is calculated as 2−800 s^{-1} when [EF2] = 0.5−20 μM, using a k_{on} of 4×10^6 s^{-1} M^{-1}, as obtained for EF1 binding to immobilized EF2. In addition, k_{app} was almost independent of the EF2 mutations, indicating that the rate-limiting step was a process not involving EF2 at all. Instead, we believe that the rate-limiting step is dissociation of dimers of immobilized EF1. In solution, EF1 forms homodimers in the presence of Ca^{2+} with an equilibrium association constant of 2×10^5 M^{-1} (unpublished data). In the flexible dextran matrix, the local concentration of EF1 may be fairly high, and the dissociation of the EF1−EF1 complex has to precede the formation of the EF1−EF2 complex. The dissociation rate constant of the EF1−EF1 homodimer has previously been estimated to be 4.9×10^{-3} s^{-1}, using SPR technology with EF1 as both the immobilized and mobile ligand (E. Thulin C. A. K. Borrebæck, A.-C. Malmborg, and S. Forsén, personal communication). This number is in very good agreement with a k_{app} of $\approx 4.5 \times 10^{-3}$ s^{-1} obtained here, and supports our interpretation of the association data.

The fact that k_{on} could not be measured for EF2 binding to immobilized EF1 was a disappointment, and the equilibrium association constants could not be calculated. However, the same problem may occur in a solution experiment, because even there homodimers need to dissociate before a heterodimer can be formed.

Fluorescence Spectroscopy. Association between wt-EF1 and wt-EF2 was studied using fluorescence spectroscopy, using the single tyrosine in EF1 as a reporter of complex formation. Association between wt-EF1 and F66W-EF2 was studied using the tryprophan in F66W-EF2 as a reporter of complex formation. In both sets of experiments, the change in fluorescence was linear with added fragment until the 1:1 stoichiometry point was reached, after which no further change was seen (data not shown). Attempts to fit the data could only yield a lower limit to the association constant ($K_A \geq 10^{10}$ M^{-1}). Fluorescence titrations could therefore not be used to compare the mutated fragments with wild-type fragments, because the requirement for using lower peptide concentrations would reduce the signal-to-noise ratio below a reasonable value. Instead, the ability of each EF2 variant to compete with F66W for binding to wt-EF1 was studied using competition experiments in which increasing amounts of EF2 variant were added to a 1:1 mixture of wt-EF1 and F66W-EF2. Each solution was allowed to equilibrate for 24 h before recording the fluorescence. On the basis of these experiments, the EF2 mutants could be divided into two groups; V61G, V61A, and F66A bound to wt-EF1 at least 2 orders of magnitude weaker than F66W, whereas the wild type, V70L, and I73V displayed affinities similar to that of F66W. Although less precise than the SPR results, the fluorescence data confirm these results in terms of the ranking of the mutants.

DISCUSSION

The association rate constants for binding of ligands to proteins vary considerably, depending on the sizes of the interacting molecules, on the existense of steering forces, and on conformational changes that take place upon binding. Many small molecules are found to bind very rapidly, at rates approaching those expected for diffusion-controlled processes. In such cases, SPR is not a suitable method for studying association rates, since the concentration of the ligand in the mobile phase close to the immobilized molecules will be lower than in the bulk during the initial fast association process and thus not constant during the experiment. Typical on rates in the diffusion-controlled limit are $\sim 10^9$ M^{-1} s^{-1} for small proteins and ligands. Such high on rates require every encounter to lead to complex formation and are only observed in a few systems where, for example, strong electrostatic attraction favors formation of productive reaction complexes. In contrast, many protein−protein interactions occur without any specific steering forces and are characterized by association rate constants in the range of $0.5-5 \times 10^6$ M^{-1} s^{-1} (*25*). The association rate constant, which is obtained for wild-type EF1 binding to immobilized wild-type EF2 ($k_{on} = 10^6$ M^{-1} s^{-1}), is found in this range, suggesting that only a small fraction of the EF1−EF2 encounters lead to complex formation.

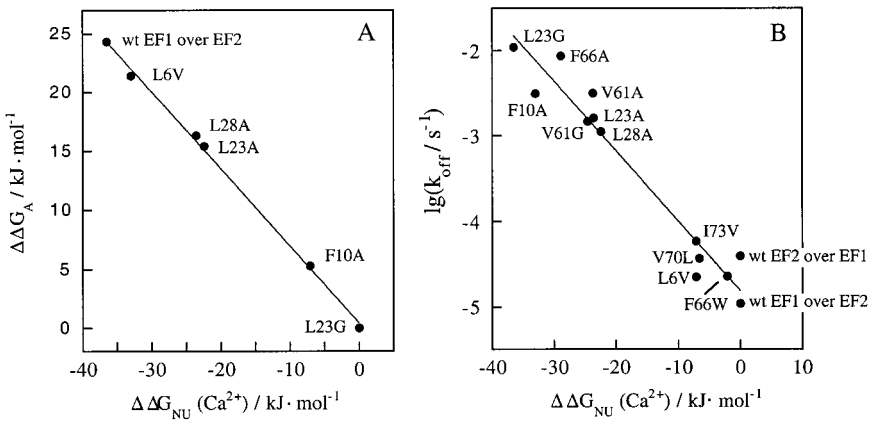

FIGURE 6: Correlation of the effect of each mutation on the affinity, K_a, or dissociation rate constant, k_{off}, and the effect on the free energy of unfolding, ΔG_{NU}, of the intact protein. (A) Effect on free energy of association $\Delta\Delta G_A$ [$=-RT \ln(K_{A,mutant}) + RT \ln(K_{A,wt})$] vs the change in stability of the Ca^{2+} form upon mutation, $\Delta\Delta G_{NU}(Ca)$. (B) Log k_{off} vs the change in stability of the Ca^{2+} form upon mutation, $\Delta\Delta G_{NU}$-(Ca). The solid lines were obtained by linear least-squares fitting to the data. The correlation coefficients are 0.999 and 0.970, respectively.

Tightly Interacting EF-Hands. A strong preference for heterodimers over homodimers has been demonstrated for the EF-hands of calbindin D_{9k} using ion exchange chromatography, agarose gel electrophoresis, and NMR spectroscopy (*15*). The affinity between the two EF-hands is impressively high in the presence of calcium ($K_A = 3.5 \times 10^{11}$ M^{-1} or $K_D = 3$ pM), and the corresponding free energy of dissociation of the EF1−EF2 heterodimer is 66 kJ mol^{-1}. The free energy of dissociation of the subdomain fragments may represent a lower limit of the free energy of unfolding of the intact protein. For the calcium form of calbindin D_{9k}, the latter is hard to obtain from denaturation studies because the protein is so stable that it does not denature even in 10 M urea at 90 °C. It is possible to estimate the free energy of unfolding of a protein from the rate of backbone amide exchange for the most slowly exchanging residue (*17*). If we do the same operation for the apo state [lowest NH exchange rate k_{ex} is 8×10^{-5} s^{-1} (*18*)], we end up with a free energy of unfolding of 31 kJ mol^{-1}, not far from what is estimated through extrapolation from a high urea concentration [27 kJ mol^{-1} (*7*)]. Calcium-bound calbindin D_{9k} is even in this case in the extreme regime. The backbone NH with the lowest exchange rate does not exchange to any observable extent during half a year, and the exchange rate can only be given as $<6 \times 10^{-9}$ s^{-1}. This gives a lower limit to the free energy of unfolding as 55 kJ mol^{-1}. If we do the backward operation, using the free energy of fragment dissociation, 66 kJ mol^{-1}, we expect an NH exchange rate of 8×10^{-11} s^{-1}, or an NH half-life of 420 years. In conclusion, calcium-loaded calbindin D_{9k} is so stable it never opens during any practical time span.

Effect of Hydrophobic Core Mutations on the Affinity between the Two EF-Hands. Most of the hydrophobic core mutations have a significant effect on the rates of association and dissociation of the two EF-hands, and also on the equilibrium affinity. Those mutations causing large changes in the side chain volumes have a large influence on the rates and affinity. The data in Tables 1 and 2 show a general trend in which changing a residue to one with a smaller side chain leads to a lower affinity and a higher off rate. In contrast, a mutation that causes an increase in the size of a side chain results in a higher affinity and a lower off rate between the two EF-hand fragments. As an example, the Phe66 → Trp substitution results in a lower off rate, whereas mutating the same residue to Ala leads to a higher off rate. For L23A and L23G, the same residue was mutated to Ala and Gly, respectively, resulting in gradually lower affinity. The relative difference in the dissociation rate constants of V61G and V61A is surprising. Contradictory to what would be expected, the Val to Ala mutation has a greater effect on the dissociation rate constant than the more extensive Val to Gly mutation. Similarly, striking results were found for the effect on the Ca^{2+}-binding cooperativity; V61G was found to have higher cooperativity between the Ca^{2+} sites than the wild-type calbindin D_{9k}, while the cooperativity of V61A was greatly impaired (*9*). On one hand, Val61 is located in the small β-sheet between the two Ca^{2+} sites, so it may not seem surprising that a mutation in this region affects the interaction between the two EF-hand subdomains. On the other hand, it is surprising that Gly61 is more easily accommodated than Ala61. A possible explanation can be found in the ability of glycine residues to adopt more different conformations than other residues, and this may restore a favorable interaction between the loops.

The amino acid sequences of human, bovine, porcine, rodent, and murine calbindin D_{9k} show that the protein is well conserved between species (Figure 2). The few amino acid substitutions that occur are in most cases very conservative. The entire hydrophobic core is identical between cows and humans, except for the L to I difference at position 32. This very high level of conservation suggests that the structural integrity of the hydrophobic core is very important for the function of calbindin D_{9k}. It has indeed been shown that the hydrophobic core substitutions that we here find to have a large influence on the affinity between the two EF-hands also affect significantly the Ca^{2+} binding properties of the protein (*9*). Of the side chains mutated in the study presented here, F10, L23, L28, V61, and F66 are conserved in all five species. L6, V70, and I73 are conserved in humans, cows, and pigs, whereas in the rodent and murine compounds, the amino acid at positions 6, 70, and 73 are E, F, and L, respectively. It is, therefore, not surprising that the effects on both stability and dissociation rates are smaller for substitutions involving L6, V70, and I73 than for those involving F10, L23, L28, V61, and F66.

Correlation between Affinity and Stability. The effects on the affinity between the two EF-hands [$\Delta\Delta G_A = -RT \ln(K_A)$] as well as the dissociation rate constants of the

bimolecular EF1−EF2 complexes (k_{off}) were compared to the effects of the same mutations on the free energy of unfolding of the intact protein $\Delta\Delta G_{NU}$ (*7*, *9*). Each intact protein used in the comparison contains the Pro43 → Met substitution in addition to the hydrophobic substitution. As seen in Figure 6, there is a strong correlation ($r = 0.999$) between $\Delta\Delta G_A$ and $\Delta\Delta G_{NU}$ for the calcium form. Likewise, a correlation ($r = 0.970$) is seen between $\log(k_{off})$ and $\Delta\Delta G_{NU}$ for the calcium form. These correlations are statistically significant with a p of <0.01. When compared to the stability parameters measured for the apo form, the correlation is somewhat lower ($r = 0.889$) which may be expected as the association between the EF-hands is assessed in the presence of calcium.

The observed correlations (Figure 6) suggest that the factors governing the stability of the intact protein also contribute to the affinity of the bimolecular EF1−EF2 complex. By measuring the free energy of association between wild-type and mutated fragments, one may avoid the general problem of assessing free energy effects by comparing values extrapolated from very unphysiological conditions such as high concentrations of denaturant, and often very different denaturant concentrations for the wild type and mutant. The subdomain approach is reliant on the reconstituted protein having a structure very similar to that of the corresponding intact protein, which has been found to be the case in many systems (see, for example, ref *19*). The loss of a covalent linkage often leads to destabilization for entropic reasons; cutting a bond leads to a larger increase in the number of available conformations in the unfolded state than in the native state. A similar effect was seen when instead of cutting, a loop was gradually increased in length (*20*). The entropic factor may be counterbalanced by enthalpic factors arising from an improved fit between the subdomains in cases where the original linkage imposes strain. The important feature is that the stability effect of losing a bond will be the same for the wild type and mutants so that the differences in the free energy of association between the fragments report on the interactions involving the mutated residue.

ACKNOWLEDGMENT

We thank Dr. Bertil Halle for the Levenberg−Marquardt fitting program LMFIT and for practical help in using and modifying it for this particular problem. We thank Eva Thulin and Hanna Nilsson for the expression and purification of the mutant proteins.

REFERENCES

1. Word, J. M., Lovell, S. C., LaBean, T. H., Taylor, H. C., Zalis, M. E., Presley, B. K., Richardson, J. S., and Richardson, D. C. (1999) *J. Mol. Biol. 285*, 1711−1733.
2. Bromberg, S., and Dill, K. A. (1994) *Protein Sci. 3*, 997−1009.
3. Wong, K. B., and Daggett, V. (1998) *Biochemistry 37*, 11182−11192.
4. Nishimoto, E., Yamashita, S., Szabo, A. G., and Imoto, T. (1998) *Biochemistry 37*, 5599−5607.
5. Linse, S., Voorhies, M., Norstrom, E., and Schultz, D. A. (2000) *J. Mol. Biol. 296*, 473−486.
6. Kellis, J. T., Nyberg, K., Sali, D., and Fersht, A. (1988) *Nature 333*, 784−786.
7. Julenius, K., Thulin, E., Linse, S., and Finn, B. E. (1998) *Biochemistry 37*, 8915−8925.
8. Nakayama, S., Moncrief, N. D., and Kretsinger, R. H. (1992) *J. Mol. Evol. 34*, 416−448.
9. Kragelund, B. B., Jönsson, M., Bifulco, G., Chazin, W. J., Nilsson, H., Finn, B. E., and Linse, S. (1998) *Biochemistry 37*, 8926−8937.
10. Brodin, P., and Grundström, T. (1986) *Biochemistry 25*, 5371−5377.
11. Johansson, C., Brodin, P., Grundström, T., Thulin, E., Forsén, S., and Drakenberg, T. (1990) *Eur. J. Biochem. 187*, 455−460.
12. O'Shannessy, D. J., Brigham-Burke, M., Soneson, K. K., Hensley, P., and Brooks, I. (1993) *Anal. Biochem. 212*, 457−468.
13. O'Shannessy, D. J., Brigham-Burke, M., Soneson, K. K., Hensley, P., and Brooks, I. (1994) *Methods Enzymol. 240*, 323−349.
14. Marquardt, P. R. (1963) *J. Soc. Ind. Appl. Math. 11*, 431−441.
15. Finn, B. E., Kordel, J., Thulin, E., Sellers, P., and Forsén, S. (1992) *FEBS Lett. 298*, 211−214.
16. Linse, S., Thulin, E., and Sellers, P. (1993) *Protein Sci. 2*, 985−1000.
17. Hvidt, A., and Nielsen, S. O. (1966) *Adv. Protein Chem. 21*, 287−386.
18. Linse, S., Teleman, O., and Drakenberg, T. (1990) *Biochemistry 29*, 5925−5934.
19. Shaw, G. S., and Sykes, B. D. (1996) *Biochemistry 35*, 7429−7438.
20. Nagi, A. D., and Regan, L. (1997) *Folding Des 2*, 67−75.
21. Svensson, L. A., Thulin, E., and Forsén, S. (1992) *J. Mol. Biol. 223*, 601−606.
22. Koradi, R., Billter, M., and Wüthrich, K. (1996) *J. Mol. Graphics 14*, 51−55.
23. Richards, F. M. (1958) *Proc. Natl. Acad. Sci. U.S.A. 44*, 162−166.
24. Tanuchi, H., Parr, G. R., and Juillerat, M. A. (1986) *Methods Enzymol. 131*, 185−217.
25. Northrup, S. H., and Erickson, H. P. (1992) *Proc. Natl. Acad. Sci. U.S.A. 89*, 3338−3342.
26. Linse, S., Thulin, E., Gifford, L. K., Radzewsky, D., Hagan, J., Wilk, R. R., and Åkerfeldt, K. S. (1997) *Protein Sci. 6*, 2385−2396.

BI0014812